

Old-Population Hypervelocity Stars from the Galactic Center: Limits from the SDSS

Juna A. Kollmeier¹, Andrew Gould², Gillian Knapp³, and Timothy C. Beers⁴

ABSTRACT

We present limits on the ejection of old-population HVS from a sample of over 290,000 stars selected from the SDSS. We derive the speed at the solar circle from the measured positions and radial velocities by assuming a radial orbit and adopting a simple isothermal model of the Galactic halo, which enables us to identify candidate bound and unbound ejectees. We find 4 candidate bound F-stars from this sample, all with negative Galactocentric radial velocity (i.e., returning toward the GC). We additionally find 2 candidate unbound stars (one F and one G), however, existing proper motion measurements make these unlikely to be emerging from the GC. These data place an upper limit on the rate of ejection of old-population stars from the GC of $\sim 45 \text{ Myr}^{-1}$. Comparing to the rate for more massive B-star ejectees of $\sim 0.5 \text{ Myr}^{-1}$, our limit on the rate of ejection of old-population HVS shows that the mass function at the GC is not bottom-heavy and is consistent with being normal. Future targeted surveys of old-population HVS could determine if it is indeed top-heavy.

1. Introduction

The search for hypervelocity stars (HVS) in the stellar halo was originally proposed in order to indirectly probe the Galactic Center (GC) at optical wavelengths (Hills 1988). These stars, having been ejected from the GC via binary-exchange collisions with a putative supermassive black hole at speeds in excess of Galactic escape would provide the dynamical “smoking gun” evidence for such an object at a time when direct detection seemed remote.

¹Observatories of the Carnegie Institution of Washington, 813 Santa Barbara Street, Pasadena, CA 91101

²Department of Astronomy, The Ohio State University, 4051 McPherson Laboratory, Columbus, OH, 43210

³Department of Astrophysical Sciences, Princeton University, Peyton Hall, Princeton, NJ 08544

⁴Department of Physics & Astronomy; CSCE:Center for the Study of Cosmic Evolution and JINA: Joint Institute for Nuclear Astrophysics, Michigan State University, E. Lansing, MI 48824 USA

Despite the tremendous advances in infrared instrumentation in the intervening two decades (and the associated confirmation of the supermassive black hole at the GC), it remains extraordinarily difficult to see any but the brightest, youngest stars at the center of the Galaxy (e.g. Genzel et al. 1997; Ghez et al. 1998, 2000; Schödel et al. 2002). The existence of these young stars is a major mystery since one would naively expect that the conditions near a supermassive black hole are sufficiently hostile to prevent in situ star formation of any kind. A key question is whether or not these stars represent the “tip of the iceberg” in an otherwise normal star forming region or whether star formation is fundamentally different at the GC. Because HVS are relatively rare, it was previously not feasible to amass sufficiently large numbers of such stars to go beyond the “smoking-gun” prediction that there should be young, blue stars in the halo. In the era of deep, wide-field spectroscopic surveys, it is now conceivable to use Hills’ original idea to exploit HVS in the Galactic halo to obtain, among other things, detailed information about star formation at the GC, which is otherwise obscured from direct view, to at least a factor of 2.5 lower in mass than the young population currently being probed (Brown et al. 2005, 2008).

The Sloan Digital Sky Survey (SDSS) provides an exceptional database to search for HVS that would otherwise be missed from targeted surveys. The SDSS has obtained over 300,000 stellar spectra since it began operations (York et al. 2000; Gunn et al. 1998, 2006). The data are reduced by an automated pipeline that produces reliable spectral classifications and radial velocities (RVs). The SEGUE Stellar Parameter Pipeline (hereafter, SSPP) further processes the wavelength- and flux-calibrated spectra generated by the standard SDSS spectroscopic reduction pipeline (Stoughton et al. 2002), obtains equivalent widths and/or line indices for 82 atomic or molecular absorption lines, and estimates T_{eff} , $\log g$, and $[\text{Fe}/\text{H}]$ through the application of a number of approaches (Lee et al. 2008a,b; Allende-Prieto et al. 2008). With this enormous database of stellar spectra it is already possible to detect HVS among a broad class of stars. In particular, the size of the SDSS stellar library makes SDSS sensitive to F and G type HVS which require a substantially different search strategy than their O and B counterparts (Kollmeier & Gould 2007). In contrast to the photometric survey, the SDSS RV catalog is not complete in any dimension. In this work, we examine a large sample of high-velocity stars in order to place limits on the ejection of F/G stars from the GC.

In § 2 we will summarize the stellar spectra and the sample selection for stars that will be used for this analysis. In § 3 we present limits on the ejection of old-population HVS. We compare this limit with young-population HVS in § 4. We present our discussion and conclusions in § 5.

2. The Sample

The sample used here is part of an ongoing study to find high-velocity stars within the SDSS (Knapp et al. 2009, in preparation). All RVs for stars acquired by the SDSS as of 15 January 2007 were extracted from the SDSS database. Selected objects were required to have RV errors not exceeding 100 km s^{-1} and required to be free of pipeline flags indicating likely problems in the automated velocity determination. This yielded a sample of 291,111 objects. Velocities were converted to Galactocentric velocity assuming that the local rotation speed is 220 km s^{-1} and that the Sun moves at $(+9,+12,+7) \text{ km s}^{-1}$ relative to the local standard of rest in the direction of the GC, Galactic rotation and the north Galactic pole respectively. All objects with Galactocentric RVs in excess of $|V_G| \geq 350 \text{ km s}^{-1}$ were examined to ensure the sample was free of catastrophic velocity errors. This process yielded a total sample of 33 objects with Galactocentric RVs exceeding $\pm 400 \text{ km s}^{-1}$, which we analyze in detail below.

3. F and G Star Ejectees

Kollmeier & Gould (2007) argued that large RV samples, such as SDSS, could probe an as yet undiscovered old population of stars ejected from the GC and would be most sensitive to stars near the main-sequence turnoff within this population. Moreover, they argued that such surveys would be more sensitive to the bound rather than unbound members of this population, simply because the bound stars accumulate over the lifetime of the Galaxy and can be seen still orbiting, while the unbound stars can only be viewed during their exit. In this section, we analyze the sensitivity of SDSS to both classes of ejectees, and we tabulate the candidates derived from this database.

3.1. Selection Criteria for Bound Ejectees

We begin by asking what the sensitivity of the SDSS survey is to bound turnoff stars and whether any such candidates are in the sample. Of course, this requires that we establish selection criteria that remove the vast majority of contaminants but still retain significant sensitivity to bound ejectees. We adopt the following two criteria:

$$v_{r,G} > v_{\text{cut}} = 400 \text{ km s}^{-1}, \quad v_{\odot\text{-circle}} < v_{\text{esc}}, \quad (1)$$

where $v_{r,G}$ is the observed RV converted to the Galactic frame, $v_{\odot\text{-circle}}$ is the velocity that the star has when it crosses the solar circle, and v_{esc} is the Galactic escape velocity, again measured at the solar circle.

The first criterion is purely observational (apart from the implied assumption of solar motion) and is self-contained. The threshold v_{cut} is established empirically from the observed velocity distribution (Knapp et al. 2009, in prep). The second criterion requires that we specify both a model of the Galaxy (to determine the value of v_{esc}) and a model of the photometric properties of the target population (ejectees), so that we can estimate $v_{\odot\text{-circle}}$ from its observed $v_{r,G}$ and from the observed fluxes in several bands.

For the Galactic model, we adopt an isothermal sphere characterized by a rotation speed $v_c = 220 \text{ km s}^{-1}$, truncated at a Galactocentric radius R_b . For this model $R_b = R_0 \exp[(v_{\text{esc}}/v_c)^2/2 - 1]$. We will adopt $v_{\text{esc}} = 550 \text{ km s}^{-1}$, which implies $R_b = 8.37 R_0$, as a default, but will also consider other values. We will consider two classes of stars, ‘F stars’, defined observationally as $0.3 < (g-i)_0 \leq 0.5$, and ‘G stars’, defined as $0.5 < (g-i)_0 \leq 0.75$. We adopt for these absolute magnitudes $M_g = 3.5$ and $M_g = 5.5$, respectively. It is important to keep in mind that these assumptions apply only to the putative ejectee population: the photometric properties of non-ejectee stars, which obviously dominate the SDSS sample overall, are completely irrelevant.

From the observed dereddened magnitude g_0 of the star, we can then infer its distance, $r = 10^{(g_0 - M_g)/5 - 2} \text{ kpc}$, and hence (from its position on the sky), infer the angle ϕ between the Sun and the GC, as seen from the star. Then, since the ejectee is assumed to be on a radial orbit, its full 3-D velocity is $v = |v_{r,G} \sec \phi|$, and hence its velocity at the solar circle (assuming, as is always the case for F stars in SDSS, that $R < R_b$) is

$$v_{\odot\text{-circle}} = \sqrt{(v_{r,G} \sec \phi)^2 + 2v_c^2 \ln(R/R_0)}. \quad (2)$$

It is immediately obvious that this equation places strong constraints on the observational parameter space in which the search can be conducted. For instance, if the star is fairly bright, so that $r \ll R_0$, then $\cos \phi > v_{\text{cut}}/v_{\text{esc}}$. Since, for this geometry, $\cos \phi \sim -\cos l \cos b$, this constraint eliminates the roughly $v_{\text{cut}}/v_{\text{esc}} = 73\%$ of the sky that is not sufficiently close to the Galactocentric (or anticentric) directions. At the opposite extreme, a bound star at $R > R_0 \exp[(v_{\text{esc}}/v_{\text{cut}})^2/2] \sim 2.57 R_0$ cannot be probed in any direction because its velocity (and hence RV) will fall below the threshold. At intermediate distances, these two effects combine with different relative weights.

3.2. Candidate Bound Ejectees

Of the stars in the Knapp et al. (2009) sample, four F stars (and no G stars) survive as candidate bound ejectees (see Table 1). It is a curious fact that all four are coming toward us, however there is a 1/8 random probability that all four would be going in the

same direction, which is too high to warrant further analysis. It is also interesting that these stars are all measured to be metal poor. These candidates could either be members of a metal-poor population ejected from the GC or simply halo stars. Obtaining proper motion measurements for the candidates would discriminate between the two scenarios.

3.3. General Formulae for Bound-Ejectee Sensitivity

Initially, consider a spectroscopic survey that obtains RVs of all stars in a small angular area Ω over a narrow magnitude range $g_0 \pm \Delta g_0/2$, and over a specified narrow range of colors. Consider a star in this sample that is ejected from the GC, with current Galactocentric RV v_r , and assume that it has an absolute magnitude (estimated from its color) M_g . The star then has distance from us $r = 10^{(g_0 - M_g)/5 - 2}$ kpc, so the volume of such a survey is

$$\Delta V = \frac{\ln 10}{5} \Delta g_0 \Omega r^3. \quad (3)$$

As mentioned above it has a 3-D Galactocentric velocity $v = v_r \sec \phi$, where ϕ is the angle between us and the GC, as seen from the star.

As seen from the GC, the probed volume covers an area ΔA and has a thickness Δw . Of course, $\Delta V = \Delta A \Delta w$. A fraction $\Delta A/4\pi R^2$ of all ejected stars will pass through this volume at some time (assuming isotropic ejection), where R is the star's Galactocentric distance, and it will spend a fraction $2\Delta w/vP$ of its time in this volume, where P is the orbital period. Hence, observations of this volume will probe a fraction

$$f_{\text{vol}} = \frac{\Delta A}{4\pi R^2} \frac{2\Delta w}{vP} = \frac{\ln 10}{2.5} \frac{\Delta g_0 \Omega r^3}{4\pi R^2 v P} \quad (4)$$

of all ejected stars. Now consider that we do not observe all stars in this volume, but only one. Clearly, the fraction of ejected stars that we probe falls by a factor N_{vol} , where N_{vol} is the number of stars that satisfy our detection criteria. That is, $N_{\text{vol}} = n\Omega\Delta g_0$, where n is the number density of stars per steradian, per magnitude, and satisfying the color criteria. Hence, the fraction of all ejected stars probed by this single observation of the i th star is

$$f_i = \frac{\ln 10}{2.5} \frac{r_i^3}{4\pi R_i^2 v_i P_i n_i}. \quad (5)$$

To determine the period, we apply our adopted Galactic model, first finding that the apocenter of the orbit R_m will be

$$R_m = R_*, \quad (R_* \leq R_b); \quad R_m = \frac{R_b}{1 + \ln(R_b/R) - (v/v_c)^2/2} \quad (R_* > R_b) \quad (6)$$

where

$$R_* \equiv R \exp \frac{(v/v_c)^2}{2}. \quad (7)$$

The velocity v' at any point in the orbit R' will be given by

$$\frac{1}{2} \left(\frac{v'}{v_c} \right)^2 = \ln \frac{R_*}{R'}, \quad (R' \leq R_b); \quad \frac{1}{2} \left(\frac{v'}{v_c} \right)^2 = \frac{R_b}{R'} - \frac{R_b}{R_m}, \quad (R' > R_b). \quad (8)$$

Integrating the equation $dt = dR'/v'(R')$ over one full period yields

$$P = \sqrt{2\pi} \frac{R_*}{v_c}, \quad (R_* \leq R_b), \quad (9)$$

$$P = \sqrt{2\pi} \frac{R_*}{v_c} \operatorname{erfc} [\sqrt{\ln(R_*/R_b)}] + \sqrt{2} \frac{R_m}{v_c} \left[\sqrt{1-x} + \frac{\arccos \sqrt{x}}{\sqrt{x}} \right], \quad (R_* > R_b) \quad (10)$$

where $x \equiv R_b/R_m$.

The total sensitivity of the survey is then simply the sum $f_{\text{tot}} \equiv \sum_i f_i$ over all stars. If there are N_{tot} bound stars orbiting, then the expected number of detections will simply be $N_{\text{exp}} = f_{\text{tot}} N_{\text{tot}}$. It will prove useful later on to express the same result as

$$\Gamma_{\text{thresh}}^{-1} = \tau_{\text{MW}} \sum_i f_i, \quad (11)$$

where $\tau_{\text{MW}} = 10$ Gyr is the lifetime of the Milky Way. In this formulation, $N_{\text{exp}} = \Gamma/\Gamma_{\text{thresh}}$, where Γ is the mean bound-ejection rate averaged over the lifetime of the Galaxy.

To understand the basic properties of f_i , let us initially restrict attention to the first case, $R_* \leq R_b$. Then

$$f_i = \frac{\ln 10}{5} (2\pi)^{-3/2} \left(\frac{r_i}{R_i} \right)^3 \frac{\exp(-z^2/2)}{zn_i}, \quad z \equiv \frac{v}{v_c} \quad (12)$$

If we consider some typical values for relatively faint turnoff stars in SDSS ($g_0 \sim 18.5$), $r \sim 10$ kpc, $R \sim 16$ kpc, $z = 2$, and $n = 100 \text{ deg}^{-2}$, then $f_i \sim 1.5 \times 10^{-9}$. Hence, by obtaining RVs for about 10^4 stars, one could probe a bound population of F stars ejected from the GC provided it had at least 10^5 members. This corresponds to $\Gamma_{\text{thresh}} = 10 \text{ Myr}^{-1}$.

3.4. Bound-Ejectee Sensitivity of SDSS

To determine the sensitivity of the SDSS spectroscopic survey, we first evaluate n_i for our two classes of stars as a function of magnitude and position on the sky using the SDSS

photometric catalog. This was done using 20 individual patches of sky, each with area 1 square degree, and interpolating these values to obtain n_i for other parts of the sky. We then sum equation (5) over all stars in the SDSS spectroscopic catalog that meet our color criteria. Figure 1 shows the result for several cases. The three bold curves (blue) are for F stars under the assumption of $v_{\text{esc}} = 550 \text{ km s}^{-1}$ and for three different thresholds, $v_{\text{cut}} = 400, 410, \text{ and } 420$. The solid (red) curve is for F stars with $v_{\text{cut}} = 400 \text{ km s}^{-1}, v_{\text{esc}} = 520 \text{ km s}^{-1}$, while the dashed (green) curve is for G stars with $v_{\text{cut}} = 400 \text{ km s}^{-1}, v_{\text{esc}} = 550 \text{ km s}^{-1}$. The two other curves will be explained later.

Several features are apparent from this figure. First, sensitivity is peaked quite close to the escape velocity. This may seem surprising in view of equation (12), which exponentially declines with the square of the velocity for $R_* < R_b$, and then even more steeply. However, at low v , distant (i.e., faint) stars do not contribute because their declining speeds at large R bring them below the first selection cut in equation (1). Most distant stars gain by r^3 in equation (12), at least for $r < R_0$. Second, sensitivity falls quite steeply with increasing v_{cut} , approximately a factor 2 for each 10 km s^{-1} . This is basically a consequence of the same volume effect just analyzed. The same effect also accounts for the dramatic falloff in sensitivity if the escape velocity proves lower than our default $v_{\text{esc}} = 550 \text{ km s}^{-1}$. Finally, sensitivity to bound G-star ejectees is about 1/3 that of F stars.

Let us initially adopt the extremely simple model that the number of bound F-star ejectees is uniform as a function of $v_{\odot\text{-circle}}$. Under this assumption, we can make one test of the plausibility of the candidate population by plotting their cumulative distribution, which is shown in Figure 2. The match is extremely good.

Let us then tentatively assume that the candidates are really bound ejectees. Integrating under the entire (upper-blue) curve in Figure 1 yields $\int dv \Gamma_{\text{thresh}}^{-1} = 4.0 \text{ Myr} \cdot \text{km s}^{-1}$. However, from Figure 1 and especially Figure 2, it is clear that about 75% of this sensitivity comes from the roughly 35 km s^{-1} interval in which the four candidates are detected. Therefore, if these candidates are accepted as real, we can infer an ejection rate

$$\Gamma \sim \frac{4}{\langle \Gamma_{\text{thresh}}^{-1} \rangle} = 4 \frac{35 \text{ km s}^{-1}}{0.75 \times 4 \text{ Myr}^{-1} \cdot \text{km s}^{-1}} \sim 45 \text{ Myr}^{-1} \quad (505 \text{ km s}^{-1} < v_{\odot\text{-circle}} < 540 \text{ km s}^{-1}) \quad (13)$$

Of course, if some or all of the candidates are later vetted and found wanting, the smaller number of detections would then yield an analagous upper limit.

Since the G-star sensitivity is smaller and we find no candidates, the G stars are consistent with a similar rate, but with weaker statistics.

3.5. Unbound Ejectees

We select candidate unbound ejected stars with exactly the criterion as bound stars (eq. [1]), except reversing the sign on the second condition, $v_{\odot\text{-circle}} \geq v_{\text{esc}}$, and of course demanding that they be exiting rather than entering the Galaxy. Then, following a very similar derivation to the one given for equations (5) and (11), we immediately derive their analogs for the unbound case,

$$\Gamma_{\text{thresh}}^{-1} = \sum_i t_i \quad t_i = \frac{\ln 10}{5} \frac{r_i^3}{4\pi R_i^2 v n_i}. \quad (14)$$

This quantity is shown in Figure 1 as a function of $v_{\odot\text{-circle}}$ for F stars (bold dashed, magenta) and G stars (dotted, cyan) for the case $v_{\text{esc}} = 550 \text{ km s}^{-1}$, $v_{\text{cut}} = 400 \text{ km s}^{-1}$. Nothing prevents us from evaluating equation (14) even below v_{esc} , and we display the extensions of these curves in Figure 1. Their physical meaning is that it is possible to detect bound ejectees during their first orbit, and for orbital times of order or longer than τ_{MW} , this is actually a more accurate representation of the detection rate than averaging over a full orbits. Thus, the bound rate is really the maximum of the bound curve and extension of the unbound curve.

There is one F star candidate that survives our selection criteria and one G star. The proper motions for both of these stars are inconsistent with a Galactocentric origin as we now show. Were it ejected from the GC, based on its current position, a star should exhibit a proper motion in the direction

$$\tan(\theta) = \tan(l)\sin(b) \quad (15)$$

where θ is measured from Galactic north through east. The F star candidate has a measured proper motion from SDSS (Pier et al. 2003; Munn et al. 2004) of 34 mas yr^{-1} at 55° (with small errors) — significantly in conflict with the predicted value $\theta = 330^\circ$.

Unlike the F star, the G star candidate cannot be discarded based on the its proper-motion direction alone. The measured proper motion of 6 mas yr^{-1} is sufficiently small that the measured direction of 183° is poorly determined given the errors. We therefore compare the predicted and observed *vector* proper motions, which (unlike the case of the F star) require a distance estimate. From its g_0 magnitude we estimate a distance of 7.8 kpc, and it is therefore expected to be moving at 14 mas yr^{-1} at 244° . The magnitude of the vector difference of the expected and observed proper motions is 12 mas yr^{-1} , which is to be compared to the typical errors of $\sim 4 \text{ mas yr}^{-1}$ (Munn et al. 2004), making it unlikely that this star is an unbound ejectee.

Since Γ_{thresh} is essentially constant in the unbound regime at $(0.05 \text{ Myr})^{-1}$ for F stars and $(0.01 \text{ Myr})^{-1}$ for G stars, this lack of detections places an upper limit on the ejection of

unbound F and G stars of

$$\Gamma_{\text{unbound}}^F < 60 \text{ Myr}^{-1}, \quad \Gamma_{\text{unbound}}^G < 300 \text{ Myr}^{-1}, \quad (16)$$

at 95% confidence.

Equation (16) is broadly consistent with equation (13).

4. Comparison with B stars

The Brown et al. (2007) survey in essence covered an entire volume of Galaxy rather than a scattering of targets within the Galaxy, like SDSS. Thus, to calculate Γ_{thresh} one should perform a volume integral. An argument similar to the one given in § 3.3 leads to the equation

$$\Gamma_{\text{thresh}}^{-1} = \int_{\text{area-covered}} \frac{d \sin bdl}{4\pi} \int_{r_{\min}}^{r_{\max}} \frac{dr r^2}{[R(r, l, b)]^2 [v^2 - 2v_c^2 \ln(R/R_0)]^{1/2}} \quad (17)$$

where we have for convenience assumed the form of the Galactic potential within $R < R_b$. We estimate this expression for the Brown et al. (2007) survey by noting that it covered an area $\Delta\Omega = 5000 \text{ deg}^2$ and that most of the sensitivity was in regions where $R \sim r$, by adopting an average value for the velocity in the denominator of $\langle v \rangle = 600 \text{ km s}^{-1}$, and approximating $\Delta r = r_{\max} - r_{\min} = 40 \text{ kpc}$. We then obtain $\Gamma_{\text{thresh}}^{-1} = (\Delta\Omega/4\pi)(\Delta r/\langle v \rangle) = 8 \text{ Myr}$. Hence the four detections imply $\Gamma_{\text{unbound}}^B = 4\Gamma_{\text{thresh}} = 0.5 \text{ Myr}^{-1}$.

Thus, the upper limit given by equation (16) shows that F-star ejectees are no more than 100 times more common than B-star ejectees. Since F stars themselves are about 100 times more common than B stars in the Galaxy as a whole, this result is already of some interest. Nevertheless, it would certainly be better to achieve at least a few times better sensitivity.

5. Discussion

We have presented the first limit on old-population ejectees from the Galactic Center based on data obtained with the SDSS. We have shown that the ejection of F/G stars is no more than 100 times more common than O/B star ejectees. We note that this limit is obtained simply from analyzing the stellar spectra obtained by SDSS as part of its main projects, *not* via a survey designed to preferentially select these objects. Already, this limit suggests that the mass function at the Galactic center is not weighted toward low mass star

formation — a fact impossible to determine by direct imaging of the GC alone. Because these candidates are all found to be metal poor (see Table 1), they may be part of the metal-poor halo in which case, this limit is even stronger. Proper motion measurements would determine whether they are indeed ejectees from the GC and thereby make this limit more stringent. Ongoing surveys, such as the second epoch of the Sloan Extension for Galactic Understanding and Exploration (SEGUE-II), will determine conclusively if star-formation at the GC is indeed weighted heavily toward young, massive stars.

We thank Warren Brown for helpful comments on this manuscript. JAK was supported by Hubble Fellowship HF-01197 and by a Carnegie-Princeton Fellowship during this work. AG was supported by NSF grant AST-0757888. JAK and AG acknowledge the support of the Kavli Institute for Theoretical Physics in Santa Barbara during the completion of this work. T.C.B. acknowledges partial funding of this work from grants PHY 02-16783 and PHY 08-22648: Physics Frontiers Center/Joint Institute for Nuclear Astrophysics (JINA), awarded by the U.S. National Science Foundation. This research has made use of NASA’s Astrophysics Data System, of the SIMBAD data base operated at CDS, Strasbourg, France, and of the plotting and analysis package SM, written by Robert Lupton and Patricia Monger. Funding for the creation and distribution of the SDSS-I and SDSS-II Archives has been provided by the Alfred P. Sloan Foundation, the Participating Institutions, the National Aeronautics and Space Administration, the National Science Foundation, the U.S. Department of Energy, the Japanese Monbukagakusho, the Max Planck Society, and the Higher Education Funding Council of the United Kingdom. The SDSS Web site is <http://www.sdss.org/>. The SDSS is managed by the Astrophysical Research Consortium (ARC) for the Participating Institutions. The Participating Institutions are The American Museum of Natural History, Astrophysical Institute Potsdam, University of Basel, Cambridge University, Case Western Reserve University, The University of Chicago, The Chinese Academy of Sciences (LAMOST), Drexel University, Fermilab, the Institute for Advanced Study, the Japan Participation Group, The Johns Hopkins University, the Joint Institute for Nuclear Astrophysics, The Kavli Institute for Particle Physics and Cosmology, the Korean Scientist Group, Los Alamos National Laboratory, the Max-Planck-Institute for Astronomy (MPIA), the Max-Planck-Institute for Astrophysics (MPA), New Mexico State University, The Ohio State University, University of Pittsburgh, University of Portsmouth, Princeton University, the United States Naval Observatory, and the University of Washington.

REFERENCES

Allende Prieto, C., et al. 2008, *AJ*, 136, 2070

- Brown, W. R., Geller, M. J., Kenyon, S. J., Kurtz, M. J., & Bromley, B. C. 2005, ApJ,
- Brown, W. R., Geller, M. J., Kenyon, S. J., Kurtz, M. J., & Bromley, B. C. 2007, ApJ, 660, 311
- Brown, W. R., Geller, M. J., Kenyon, S. J., 2008, ApJ, in press
- Ghez, A. M., Klein, B. L., Morris, M., & Becklin, E. E. 1998, ApJ, 509, 678
- Ghez, A. M., Morris, M., Becklin, E. E., Tanner, A., Kremenek, T., 2000, Nature, 407, 349
- Genzel, R., Eckart, A., Ott, T., & Eisenhauer, F. 1997, MNRAS, 291, 219
- Gunn, J.E., et al. 1998, AJ, 116, 3040
- Gunn, J.E., et al. 2006, AJ, 131, 2332
- Hills, J. G. 1988, Nature, 331, 687
- Knapp, G.K., Javiv, L., Gould, A., Kollmeier, J.A., et al. 2009 in preparation
- Kollmeier, J.A., Gould, A., 2007, ApJ, 664, 343)
- Lee, Y. S., et al. 2008a, AJ, 136, 2022
- Lee, Y. S., et al. 2008b, AJ, 136, 2050
- Munn, J.A., et al. 2004, AJ, 127, 3034
- Pier, J.R., Munn, J.A., Hindsley, R.B., Hennessy, G.S., Kent, S.M., Lupton, R.H., and Ivezić, Z. 2003, AJ, 125, 1559
- Schödel, R. et al. 2002, Nature, 419, 694
- Stoughton, C., et al. 2002, AJ, 123, 485
- York, D. G., et al. 2000, AJ, 120, 1579

Table 1. Candidate Ejectees Satisfying Velocity Criteria

Name	V_G (km/sec)	Type	g_0	$(g - i)_0$	T_{eff} (K)	$\log(g)$	[Fe/H]	Plate/Fiber/MJD
SDSSJ061118.63+642618.5	-412.3±5.5	F	18.39	0.45	6143	4.08	-1.27	2299/488/53711
SDSSJ074557.31+181246.7	-409.0±5.9	F	18.96	0.34	6235	3.51	-1.73	2074/113/53437
SDSSJ224052.56+011332.1	-407.1±16.3	F	19.30	0.49	6168	4.02	-1.37	1101/561/52621
SDSSJ211321.02+103456.7	-404.4±17.2	F	20.07	0.35	6069	4.10	-1.91	1891/423/53238
SDSSJ111107.85+585357.2	+425.4±3.1	F	16.16	0.36	6514	3.58	-1.77	950/554/52378
SDSSJ224740.09-004451.6	+401.8±13.1	G	19.97	0.72	5518	4.17	-1.22	1901/7/53261

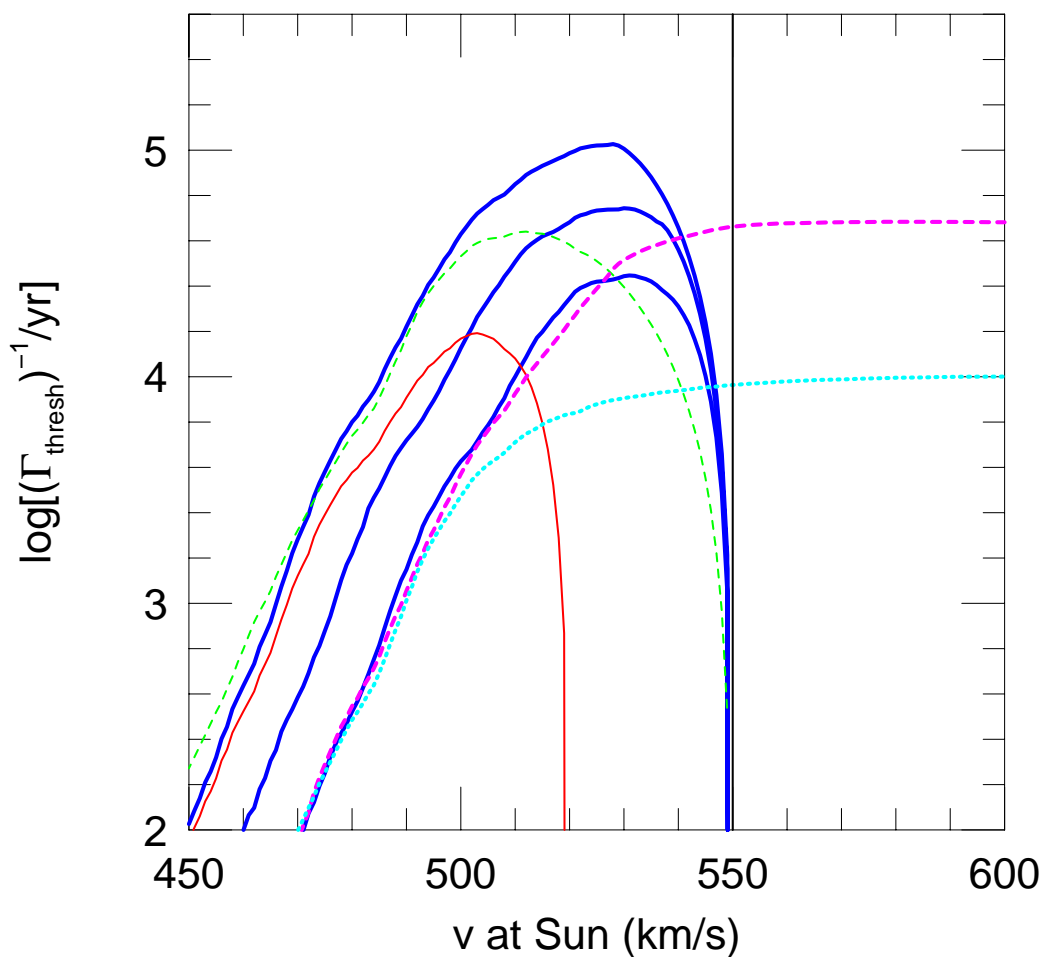


Fig. 1.— Sensitivity of SDSS to old-star ejectees as a function of type and Galactic model. Bold, blue curves show the sensitivity for bound F stars assuming $v_{\text{esc}} = 550 \text{ km s}^{-1}$ and for three different thresholds, $v_{\text{cut}} = 400, 410,$ and 420 from bottom to top. Solid red curve shows the case for bound F stars with $v_{\text{cut}} = 400 \text{ km s}^{-1}, v_{\text{esc}} = 520 \text{ km s}^{-1}$, while the dashed (green) curve is for bound G stars with $v_{\text{cut}} = 400 \text{ km s}^{-1}, v_{\text{esc}} = 550 \text{ km s}^{-1}$. The sensitivity to unbound F stars (bold dashed, magenta) and unbound G stars (dotted, cyan) for the case $v_{\text{esc}} = 550 \text{ km s}^{-1}, v_{\text{cut}} = 400 \text{ km s}^{-1}$ are also shown.

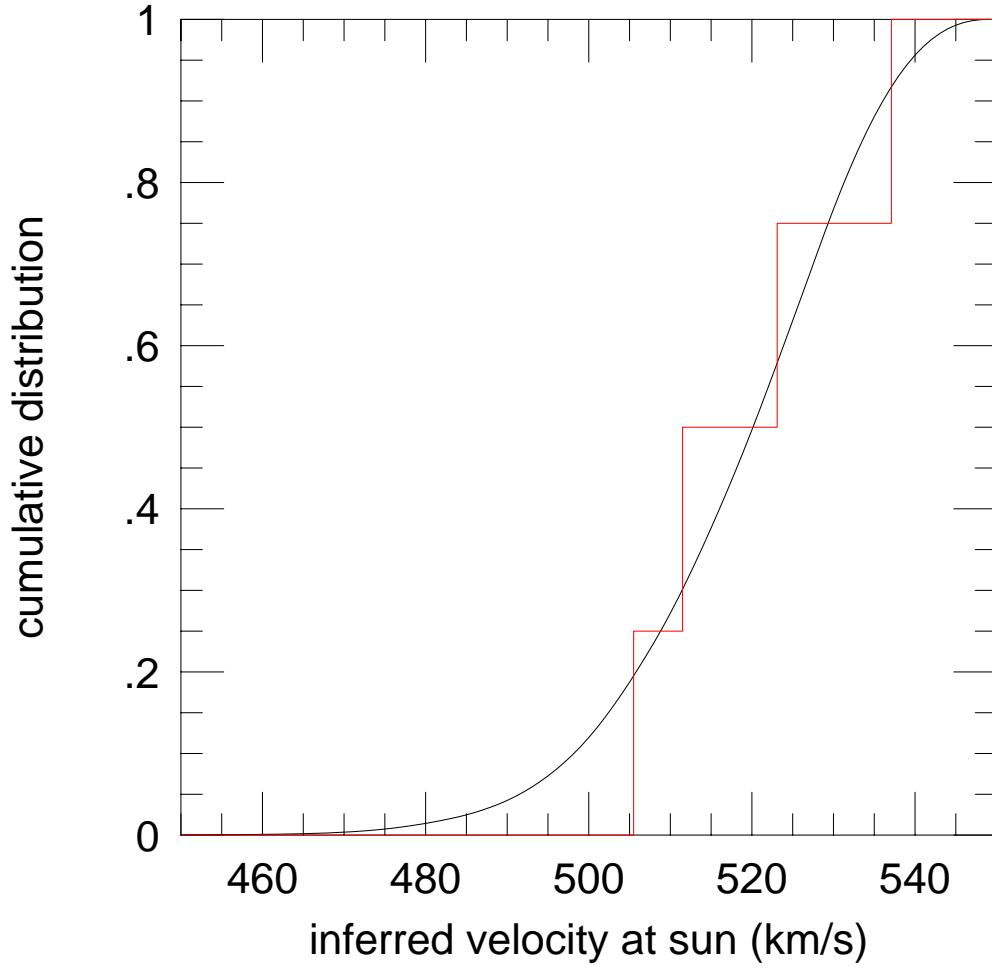


Fig. 2.— Cumulative distribution of velocities of candidate bound F-star HVS population (red histogram). A simple model in which the number of bound F-star ejectees is a uniform function of $v_{\odot\text{-circle}}$ is shown in black for comparison.